Microfluid Nanofluid (2008) 4:391–399
DOI 10.1007/s10404-007-0191-2

RESEARCH PAPER

Equivalent circuit modeling of electrokinetically driven analytical microsystems

Claudio L. A. Berli

Received: 24 April 2007 / Accepted: 5 June 2007 / Published online: 5 July 2007

Abstract Equivalent circuit modeling of microfluidic chips accounts for the transport of fluid and electricity in the entire network of microchannels as a function of the applied pressure and electric potentials. For these calculations, each microchannel is represented by a set of conductance coefficients that relates to driving forces and conjugate flows. Theoretical expressions of the coefficients for rectangular microchannels with arbitrary values of the cross-sectional aspect ratio are derived from the fundamentals of electrokinetic phenomena. Particular emphasis is placed on the analysis of the conditions under which the equivalent circuit model can be accurately employed. Model predictions successfully match data on electrokinetically driven chips for immunoassays reported in the literature. A simulation example is also given to illustrate the capability of the technique for the design and manipulation of analytical microsystems.

Keywords Microfluidics · Electrokinetic flow · Equivalent circuit models · Rectangular microchannels · Analytical chips

1 Introduction

A wide variety of analytical chips are operated by means of electrokinetic flow (Seiler et al. 1994; Chiem and Harrison 1998; Fletcher et al. 1999; Dodge et al. 2001; Chien and Bousse 2002; Hu et al. 2005). The precise manipulation of these devices requires accurate predictions of fluid flow and electric current throughout the network of microchannels. In microfluidics (Stone et al. 2004; Tabeling 2005; Squires and Quake 2005) Reynolds numbers are normally lower than 1, meaning that inertial effects are negligibly small in comparison with viscous forces. In addition, microchannels are generally thin enough to produce fully developed flows. Consequently, the relationships between driving forces (pressure, electric potential) and conjugate flows (fluid, electricity) are linear, which allows to describe microfluidic networks by analogy with electrical circuits. Simple equivalent circuits were proposed to emulate networks where physicochemical characteristics of channels and fluids are homogeneous (Seiler et al. 1994; Knight et al. 1998; Fletcher et al. 1999; MacInnes et al. 2003; Kohlheyer et al. 2005). Equivalent circuit models addressed to heterogeneous networks were also reported (Morf et al. 2001; Chien and Bousse 2002; Chatterjee and Aluru 2005), although disregarding the streaming current. In more detailed descriptions (Xuan and Li 2004; Berli 2007), each channel is represented by an appropriate set of conductance coefficients (hydraulic, electro-osmosis/streaming, electric), which are derived from the fundamentals of electrokinetic phenomena. Thus flow rate and electric current are predicted simultaneously in the entire network, in terms of applied electric potential and pressure gradients. These models are also useful to assist the design of microfluidic devices, as well as the implementation of more sophisticated numerical calculations that focus on particular regions of the system (Erickson 2005).

As it is usual in dealing with problems where the underlying physics is relatively complex, a number of assumptions are introduced in equivalent circuit modeling

C. L. A. Berli (✉)
INTEC (Universidad Nacional del Litoral-CONICET),
Güemes 3450, 3000 Santa Fe, Argentina
e-mail: cberli@ceride.gov.ar

C. L. A. Berli
Departamento de Física,
Facultad de Bioquímica y Ciencias Biológicas,
UNL, El Pozo, 3000 Santa Fe, Argentina

of microfluidic networks. Rigorously speaking, equations depict idealized microchannels and flow conditions. In this sense, the main objective of the present work is to develop analytical formulae that approximate as close as possible to real microfluidic networks, and eventually, state clearly the conditions under which the model should be employed. For the purposes, the paper consists of the following contents and organization. In Sect. 2, the derivation of equivalent circuit equations for microchannel networks is briefly described. In Sect. 3, theoretical expressions of conductance coefficients are deduced for rectangular microchannels with arbitrary values of the cross-sectional aspect ratio, and filled with electrolyte solutions of moderate ionic concentrations, which is the situation commonly found in analytical microsystems. It is worth to mention that expressions of the coefficients for cylindrical and slit micro/nanochannels were previously studied (Xuan and Li 2004; Berli 2007, and references therein). Also in Sect. 3, the theoretical basis is reviewed to better discuss the assumptions made and the corresponding limitations of the model, which is carried out subsequently in Sect. 4. Then, in Sect. 5, model predictions are cross-checked against data reported in the literature (Hu et al. 2005) on the manipulation of an electrokinetically controlled microfluidic chip for immunoassays. The aim of this work is also to illustrate the suitability of the technique to rationalize typical operations in analytical chips. Thus a double T-shaped microreactor with heterogeneous surface properties is considered in Sect. 6.

2 Equivalent circuit equations

The simultaneous flow rate Q and electric current I developed in a microchannel that contains electrolyte solution are described by Onsager relations for electrokinetic phenomena: $Q = L_{11}\,\Delta P + L_{12}\,\Delta V$; $I = L_{21}\,\Delta P + L_{22}\,\Delta V$ (De Groot 1951; Rastogi et al. 1993; Brunet and Adjari 2004). In these expressions, ΔV and ΔP are, respectively, electric potential and pressure differences between the ends of the channel. The coefficient L_{11} is the hydraulic conductance, $L_{12} = L_{21}$ represents electro-osmosis/streaming phenomena (Onsager reciprocal relation), and L_{22} comprises the electric conductance. These relations assume steady state flows, isothermal conditions, and no concentration gradients in the axial direction of microchannels (further details are given in Sect. 4).

Microfluidic networks involve several interconnected channels, as shown schematically in Fig. 1a, where indexes i and j identify branches and junctions, respectively. In practice, the flow is induced and controlled by applying a given configuration of pressures $P_i^{(j)}$ and potentials $V_i^{(j)}$ at channel ports (inlet/outlet). In order to predict the flow rate

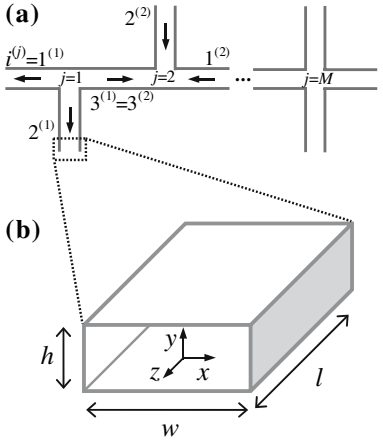

Fig. 1 **a** Plan view of a typical microfluidic network with the nomenclature that classifies branches and junctions, and the positive sign convention of the flow indicated by the *arrows*. **b** Schematic representation of a rectangular microchannel (length l, width w, depth h), and the coordinate system used in calculations

and the electric current in every $i^{(j)}$ branch of the network, one firstly needs to calculate the pressure and electric potential developed at the M junctions (Fig. 1a). For this purpose, the following conservation equations are used: $\sum_{i=1}^{N^{(j)}} Q_i^{(j)} = 0$, which derives from a simple mass balance for incompressible fluids with uniform density, and $\sum_{i=1}^{N^{(j)}} I_i^{(j)} = 0$, which establishes the electric charge conservation (Kirchoff law for circuit nodes). In these expressions, $N^{(j)}$ is the total number of branches associated to the junction j. Introducing Onsager relations for each branch yields,

$$\left.\begin{aligned} \sum_{i=1}^{N^{(j)}} L_{11,i}^{(j)}\Delta P_i^{(j)} + L_{12,i}^{(j)}\Delta V_i^{(j)} = 0 \\ \sum_{i=1}^{N^{(j)}} L_{21,i}^{(j)}\Delta P_i^{(j)} + L_{22,i}^{(j)}\Delta V_i^{(j)} = 0 \end{aligned}\right\}, \quad j = 1 \text{ to } M, \tag{1}$$

with the following definitions: $\Delta P_i^{(j)} = P_i^{(j)} - P_c^{(j)}$, $\Delta V_i^{(j)} = V_i^{(j)} - V_c^{(j)}$, for j where the flow is positive going out from the intersection; and $\Delta P_i^{(j)} = P_c^{(j)} - P_i^{(j)}$, $\Delta V_i^{(j)} = V_c^{(j)} - V_i^{(j)}$, for j where the flow is positive towards the intersection, in agreement with the sign convention defined in Fig. 1a. Here $P_c^{(j)}$ and $V_c^{(j)}$ are the pressure and potential values at junctions. These $2M$ unknowns can be determined by solving the system of $2M$ linear equations given by (1). Calculations can be carried out with standard mathematical software, by using Cramer's rule for example (e.g. Berli 2007).

Therefore, if the applied pressures and potentials are given, and the set of $3\sum_{j=1}^{M} N^{(j)}$ coefficients is known for

the system, the pressures and potentials at the junctions can be calculated, and then both Q and I are obtained for every branch in the network. In fact, the relationship between all driving forces and conjugate flows is determined by the set of coefficients entering (1). In what follows, theoretical expressions of L_{11}, L_{12}, L_{21}, and L_{22} are deduced for microchannels of rectangular cross-section (Fig. 1b), which are found in a large number of analytical microfluidic chips.

3 Conductance coefficients for rectangular microchannels

3.1 Theoretical framework

The foundations of electrokinetic flow are well documented in the literature (Probstein 1989; Hunter 1992; Li 2004). The case of microchannels filled with an electrolyte solution of Newtonian viscosity μ, density ρ, and permittivity ε is considered here. The electrostatic charges present at the solid–liquid interface involve an electrical potential that decreases steeply in the liquid due to the screening produced by dissolved counterions and other electrolyte ions, which constitute the electric double layer (EDL). Electrokinetic effects arise when there is a movement of the liquid and associated ions in relation to the solid. In the framework of continuum fluid mechanics, the fields of fluid velocity (u), pressure (p), and electric potential (ϕ) are governed by the following set of coupled equations (Stone et al. 2004; Tabeling 2005; Squires and Quake 2005),

$$\nabla \cdot \mathbf{u} = 0, \tag{2}$$

$$0 = -\nabla p + \mu \nabla^2 \mathbf{u} + \rho \mathbf{g} - \left(e \sum_k v_k n_k \right) \nabla \phi, \tag{3}$$

$$\varepsilon \nabla^2 \phi = -e \sum_k v_k n_k. \tag{4}$$

Equation (2) expresses the continuity of mass for uniform fluid density and isothermal conditions. Equation (3) is the conservation of momentum for low Reynolds numbers flow (this aspect is further discussed in Sect. 4). The last term on the right-hand side of Eq. (3) represents the contribution of electrical forces to the momentum balance, where $e \sum_k v_k n_k$ is the local charge density of the electrolyte solution, obtained as the summation over all ionic species k with valence v_k and number density n_k (e is the elementary charge). Also in Eq. (3), g is the acceleration of gravity. Equation (4) establishes the electric potential in the flow domain of the channel, which is composed of two contributions: the EDL potential and the externally applied potential.

Since ion distributions n_k are not known, they must be obtained from transport equations that account for the effect of electrical forces, fluid convection, and Brownian diffusion (Nerst-Plank equation; see, for instance, Probstein 1989). In the present work, this step is avoided by introducing a suitable simplification: the so-called thin EDL approximation. In fact, the thickness of the EDL is quantified through the Debye length, $\lambda = \left(\varepsilon k_B T / e^2 \sum_k v_k^2 n_k^{(b)} \right)^{1/2}$, where $n_k^{(b)}$ are the bulk ion densities, k_B is Boltzmann constant and T is the absolute temperature (Probstein 1989; Hunter 1992). For the ionic concentrations normally used in practice, $\lambda \approx$ 1–10 nm, while cross-sectional channel dimensions are 10–100 μm. Consequently one may assume that $\sum_k v_k n_k \approx 0$ in most of the flow domain, except in the close vicinity of charged interfaces.

3.2 Flow rate (L_{11} and L_{12})

The thin EDL approximation enables the decoupling of electric and hydrodynamic fields, which has relevant advantages for the purposes here. Firstly, as the last term on the right-hand side of Eq. (3) vanishes, the flow induced by pressure gradients in the axial direction z of the channel (Fig. 1b) is readily obtained as follows (White 1975; Brody et al. 1996; Tabeling 2005),

$$u_z^{(p)}(x,y) = \frac{4h^2}{\mu} \frac{\Delta P}{l} \sum_{m=1}^{\infty} \frac{(-1)^{m+1}}{\beta_m^3} \times \left[1 - \frac{\cosh(\beta_m x/h)}{\cosh(\beta_m w/2h)} \right] \cos(\beta_m y/h), \tag{5}$$

where $\beta_m = (2m-1)\pi$, and $\Delta P/l = \partial(p - \rho g_z z)/\partial z$ is the generalized pressure gradient for fully developed flows (it is worth noting that an equivalent expression of $u_z^{(p)}(x,y)$ is obtained by using Green's function formulation, e.g. Li 2004). Secondly, as the right-hand side of Eq. (4) also vanishes, one may write the electric field in the flow domain in terms of the externally applied potentials, that is $\partial\phi/\partial z = \Delta V/l$, which is valid for uniform ion densities along the axial direction. Then, the electrokinetic effects are taken into account separately: when $\Delta V/l$ is imposed, the electric forces acting on excess ions in the EDL drag the surrounding liquid, and thus electro-osmosis takes place. The shear is confined to thin layers (of the order of λ) adjacent to solid–liquid interfaces, where the electric potential is designated ζ-potential. For this reason, the effect is regarded as an electrically induced slip velocity in the direction of the field, the magnitude of which is (Probstein 1989; Hunter 1992; Li 2004)

$$u_z^{(e)} = -\frac{\varepsilon\zeta}{\mu}\frac{\Delta V}{l}. \tag{6}$$

Therefore, the electrokinetic flow profile is $u_z(x,y) = u_z^{(p)}(x,y) + u_z^{(e)}$, where the components are given by Eqs. (5) and (6), respectively. Integrating $u_z(x,y)$ in the cross-sectional area of the channel (Fig. 1b) yields $Q = L_{11}\,\Delta P + L_{12}\,\Delta V$ with the following coefficients:

$$L_{11} = -\frac{wh^3}{12\mu l}\sum_{m=1}^{\infty}\frac{96}{\beta_m^4}\left[1 - \frac{\tanh(\beta_m w/2h)}{\beta_m w/2h}\right], \tag{7}$$

$$L_{12} = \frac{wh\,\varepsilon\,\zeta}{\mu\,l}. \tag{8}$$

An interesting feature is that the series in Eq. (7) converges to 1 for large values of w/h, namely the sum reaches 0.99 for w/h around 60. In this limit, $L_{11} \approx -wh^3/12\mu l$, in agreement with the well known hydraulic conductance of slits (planar Poiseuille flow). Also L_{12}, which is independent on the ratio w/h, coincides with the respective coefficient for slit microchannels (e.g. Berli 2007, and references therein).

3.3 Electric current (L_{21} and L_{22})

The transport of electricity in the flow domain also involves two contributions: $I = I^{(p)} + I^{(e)}$, which are the streaming and conductive currents, respectively (Probstein 1989; Hunter 1992; Li 2004). In fact, when a shear flow is established on a charged interface (in this case due to the pressure-driven fluid velocity $u_z^{(p)}$), the convective transport of ions in the EDL produces a surface current in the direction of the flow. Recently Brunet and Adjari (2006) suggested an elegant procedure to deal with streaming effects under the thin EDL approximation: for relatively small λ in relation to channel cross-sectional size, the effective streaming current is confined to a thin layer (of the order of λ) adjacent to the interface, and it results proportionally to the wall shear rate as,

$$J_z^{(p)} = -\varepsilon\zeta\left|\partial u_z^{(p)}/\partial x\right|_{x=w/2}. \tag{9}$$

This expression accounts for the current per unit width of the zy-plane locally tangent to the interface at $x = w/2$ (shaded wall in Fig. 1b). The current produced by that wall is obtained by integrating Eq. (9) in the y-direction over the height h. The total streaming current developed in the microchannel comprises the effect on the four walls, i.e. at $x = \pm w/2$ and $y = \pm h/2$ (Fig. 1b). Given the symmetry of the problem, and considering uniform ζ-potential,

$$I^{(p)} = -\varepsilon\zeta\left\{4\int_0^{h/2}\left|\partial u_z^{(p)}/\partial x\right|_{x=w/2}dy + 4\int_0^{w/2}\left|\partial u_z^{(p)}/\partial y\right|_{y=h/2}dx\right\}, \tag{10}$$

with $u_z^{(p)}$ from Eq. (5). In addition, the conductive current $I^{(e)}$ is obtained by integrating the bulk current density $\sigma\,\Delta V/l$ in the cross-sectional area of the channel, where $\sigma = e\sum_k v_k^2\omega_k n_k^{(b)}$ is the electric conductivity of the solution and ω_k is the ionic mobility (Probstein 1989; Hunter 1992; Li 2004).

Therefore, performing the integrations and adding both contributions yield $I = L_{21}\,\Delta P + L_{22}\,\Delta V$ with the following coefficients:

$$L_{21} = \frac{wh\,\varepsilon\,\zeta}{\mu\,l} = L_{12}, \tag{11}$$

$$L_{22} = -\frac{wh\,\sigma}{l}. \tag{12}$$

Equation (11) is an expected result taken into consideration Onsager reciprocal relations for electrokinetic phenomena (De Groot 1951; Rastogi et al. 1993). In this sense, the derivation of L_{21} could have been omitted here (Brunet and Adjari 2004). Nevertheless, according to the author's knowledge, the evaluation of streaming effects under the thin EDL approximation has not been reported before for rectangular microchannels. Further, Eq. (11) may be regarded as a consistency test for the calculations of the coefficients.

4 Assumptions made and applicability of the model

4.1 Equivalent circuit equations

Equation (1) are restricted to the following situations:

(i) steady state flow,
(ii) constant and uniform temperature,
(iii) constant and uniform fluid density,
(iv) no concentration gradients along channels,
(v) negligible hydraulic/electric resistance at junctions.

Discussing (*i*) firstly requires the introduction of Reynolds number $Re = \rho Uh/\mu$, where U is a characteristic fluid velocity, here taken as the average value in the channel cross-section. In analytical microfluidic systems, U is of the order of mm/s, hence $Re \ll 1$, meaning that the flow is controlled by viscous forces (Squires and Quake 2005; Tabeling 2005). Inertial terms were omitted in Eq. (3)

precisely for this is reason. Under the circumstances, the time required to reach the steady state after flow inception is negligible small. For $Re \sim 1$, it can be estimated as $\tau \approx \rho w^2/\mu$, which is of the order of milliseconds for aqueous solutions in micro-scale channels (Brody et al. 1996; Stone et al. 2004; Tabeling 2005). Furthermore, a recent work on the starting profile of electro-osmotic velocity reports that $\tau \rightarrow 0$ as $Re \rightarrow 0$ (Zhou et al. 2006). Therefore, in a practical sense, the electrokinetic flow is steady during typical operations that take several seconds, like sample injection, reaction, and separation in analytical microsystems. This was nicely shown by Brody et al. (1996), who demonstrated experimentally that the fluid can be switched from one channel to another on a milliseconds time scale.

In relation to (*ii*), it is known that an important effect associated with electric current in microchannels is temperature rising due to internal heat generation, namely Joule effect. Extensive discussions of this effect are given in the text of Li (2004). Nevertheless, if the applied electric field is relatively low, and the microfluidic chip is able to reject the heat to the environment, the fluid temperature does not change appreciably. In order to accomplish this, field strengths lower than 300 V/cm are normally used in practice (Morf et al. 2001, MacInnes et al. 2003; Hu et al. 2005).

Conditions (*iii*) and (*iv*) are normally attained in analytical microsystems, except in some manipulations where polymer solutions, particles, or cells are transported selectively or focused in one microchannel. In particular, when strong concentration gradients are used, a third conjugated flow (osmotic transport) must be included in the equivalent circuit equations (Rastogi et al. 1993; Brunet and Adjari 2004). The same methodology is used to solve the problem, although additional complexity arises in calculations.

Concerning assumption (*v*), one may observe that junctions are not considered in the overall resistance of the network because their interfacial area ($\sim w^2$) is much smaller than that of microchannels ($\sim wl$). In fact, the hydraulic/electric resistance of junctions can be neglected in front of that of microchannels, as long as $l/w \gg 1$. This is the reason why equivalent circuit equations do not differentiate, for example, T-shaped junctions from Y-shaped ones. In other words, network architectures are not specified in modeling. However, if channel intersections present any complex shape or internal structure that produces a relatively important resistance, they must be considered as new elements in the circuit (Brunet and Adjari 2004).

4.2 Conductance coefficients

Besides the concepts discussed earlier, the assumptions required to attain the expressions (7), (8), (11) and (12) are:

(vi) relatively thin EDL,
(vii) fully developed flow,
(viii) straight microchannels,
(ix) uniform cross-section and surface properties.

In practical terms, assumption (*vi*) means that the above expressions of L_{11}, L_{12} and L_{22} apply for micro-scale channels, filled with solutions of moderate ionic concentrations, say higher than 1 mM, which leads to values of λ smaller than $10^{-3}\ h$. This situation is commonly found in a wide variety of analytical microsystems. Nevertheless, in specific situations involving very low ionic concentrations, or in the case of nano-scale channels, where λ becomes the order of the channel depth h, Eqs. (6) and (9) do not apply any more, and the full problem must be solved to find the appropriate coefficients (e.g. Xuan and Li 2004; Berli 2007, for calculations involving cylinders and slits).

Concerning (*vii*), it should be remarked that if microchannels are sufficiently thin, flows are fully developed and two-dimensional effects are present near channel ends or intersections only. The error introduced by this assumption may be roughly quantified through the hydrodynamic entrance length $l_e \approx w(0.5 + 0.06\ Re)$ (White 1975; Brody et al. 1996; Tabeling 2005). This length is slightly higher in electro-osmotic flow (Yang et al. 2001a). In any case, provided $Re < 1$, $l_e \sim w/2$, hence the assumption of fully developed flow in microfluidics simply demands $l/w \gg 1$, in agreement with the requirement of assumption (*v*). This is normally accomplished in analytical microsystems, except in some particular architectures where branches are relatively short. In these cases, the deviations from fully developed flow in the vicinity of intersections may be accounted by introducing an effective channel length $l \pm \delta l$, where the sign of the correction δl depends on the shape of the junction and flow conditions (MacInnes et al. 2003).

The assumption of straight microchannels (*viii*) may appear rather restrictive, considering that turns, folds, and even serpentines, are included in microfluidic networks. Nevertheless, if channels are relatively thin ($l/w \gg 1$), the radii of curvature of turns are higher than w, and the flow is perfectly laminar ($Re < 1$), the hydraulic resistance is not enhanced appreciably in comparison with straight microchannels. Indeed, the hydrodynamic friction factor of a serpentine microchannel equals that of a straight microchannel of equivalent path length when $Re \rightarrow 0$ (Geyer et al. 2006). Apart from these conditions, uniform surface potential and thin EDL are required to attain the similarity of electro-osmotic velocity and electric field in arbitrary geometries (Cummings et al. 2000). In non-smooth borders, spatial changes in the electric field (as well as inertial effects if $Re > 1$) impacts on the velocity profile, and the flow is not fully developed in the curvature zone (Yang et al. 2001b; MacInnes et al. 2003).

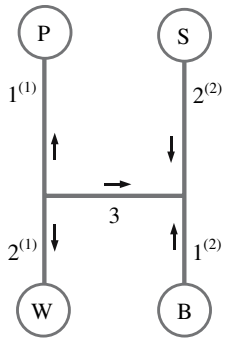

Fig. 2 Layout of the H-shaped network of microchannels composing the immunoassay chip developed by Hu et al. (2005). Cross-sectional dimensions of all channels are $h = 20$ μm and $w = 100$ μm. Channel lengths are $l_1^{(1)} = l_2^{(2)} = 14$ mm, $l_2^{(1)} = l_1^{(2)} = 9$ mm, and $l_3 = 10$ mm (the draw is not to scale). Capital letters *P*, *S*, *W*, and *B* identify the fluid reservoirs at channel ports. *Arrows* indicate the positive direction of the flow

Finally, in relation with (*ix*), it should be noted that any abrupt change in channel cross-section or surface potential must be considered as a confluence of two different branches, i.e. a new junction in the set of equations of the model (e.g. Xuan and Li 2004). In particular, slit microchannels with smooth modulations of topography or surface potential admit the calculation of conductance coefficients (Brunet and Adjari 2006).

5 Cross-checking the model against real systems

In this section the model is tested on a microfluidic chip for immunoassays developed by the Group of Li (Hu et al. 2005). The microchannel network involved is drawn schematically in Fig. 2. The surface potential is $\zeta = -18.3$ mV in all branches. The circulating fluid is an aqueous solution of Tris–HCl 25 mM, which yields $\lambda = 1.9$ nm and $\sigma \approx 0.26$ S/m. Parameters ρ, μ, and ε are those of water at 20°C. With these characteristics, and geometrical dimensions given in the legend of Fig. 2, L_{11}, L_{12}, and L_{22} were evaluated from Eqs. (7), (8), and (12), respectively, for every channel of the network. In Eq. (7), the first five terms of the series were used (the sum equals 0.874 for $w/h = 5$).

The highest Reynolds number reached in the manipulation of this device is $Re \approx 0.01$, and the lowest aspect ratio of channels is $l/w = 90$, which assure that conditions discussed in Sect. 4 are safely accomplished. Furthermore, the ratio h/λ is higher than 10^4, hence the thin EDL approximation is also amply satisfied. Under the circumstances, the equivalent circuit model can be used accurately to predict the electrokinetic flow developed in the H-shaped network during some operation steps of the immunoassay analysis.

Table 1 Average values of the fluid velocity attained in the channels of the H-shaped network shown in Fig. 2, as a function of electric potentials applied to the respective reservoirs

Operation	Reservoir	V (V)	Channel	U (μm/s)	
				Hu et al. (2005)	Model
Dispensing	P	250	$1^{(1)}$	–141	–141.4
	W	0	$2^{(1)}$	140	140.9
	S	100	$2^{(2)}$	2	2.6
	B	95	$1^{(2)}$	–3	–3.1
			3		0.5
Washing	P	0	$1^{(1)}$	102	102.3
	W	0	$2^{(1)}$	159	159.2
	S	300	$2^{(2)}$	–10	–10.7
	B	500	$1^{(2)}$	271	272.2
			3		–261.5

The sign of U is in accordance with the positive sign convention indicated by the arrows in Fig. 2

Given the potentials applied to the reservoirs P, S, W and B (Fig. 2), which are at atmospheric pressure, the flow rate and electric current in each channel were calculated. Then the average fluid velocity was obtained as $U = Q/hw$, and compared to the respective values reported by Hu et al. (2005). Results are presented in Table 1. It is worth to remark the agreement observed, taking into account that there are no adjustable parameters in calculations. Only the value of σ used is approximate; nevertheless, although crucial to determine the current, σ does not affect the flow provided it is uniform throughout the network. For the sake of brevity, only two operation steps (analyte dispensing and washing) are illustrated in Table 1. It must be mentioned however that the flows attained in all the operations performed by Hu et al. (2005) are equally well predicted by the model.

6 Case study: double T-shaped microreactors

Microchannel networks arranged in the form of a double T are usually integrated in analytical devices as microreactors (Chiem and Harrison 1998; Fletcher et al. 1999; Dodge et al. 2001; MacInnes et al. 2003). The example studied in this section (Fig. 3) is largely inspired in the chip for immunoassays reported by Dodge et al. (2001). The network is filled with an aqueous solution of KCl 25 mM, which yields $\lambda = 1.9$ nm and $\sigma = 0.37$ S/m. Channel ends are considered to be open to the atmosphere and the whole system is at 20°C. In particular, because of a surface treatment (Dodge et al. 2001), the electrokinetic potential of channels $2^{(1)}$, $2^{(2)}$, and 3, here designated ζ_{RC}, differs from that of channels $1^{(1)}$ and $1^{(2)}$, designated simply ζ

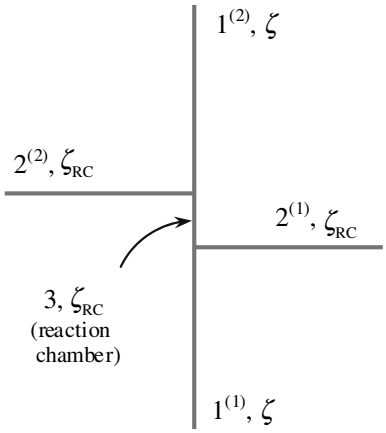

Fig. 3 Layout of a double T-shaped network of microchannels such as the microreactor integrating the microfluidic chip for immunoassays proposed by Dodge et al. (2001). Channel cross-sectional dimensions are $h = 20$ μm and $w = 50$ μm. Channel lengths were arbitrarily defined here as $l_1^{(1)} = l_2^{(1)} = l_1^{(2)} = l_2^{(2)} = 10$ mm, and $l_3 = 1$ mm (the draw is not to scale)

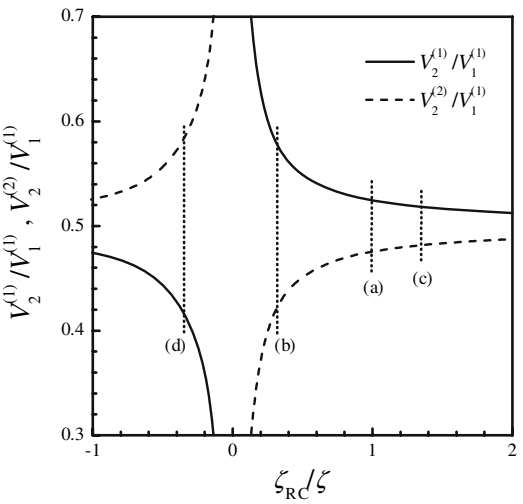

Fig. 4 Electric potentials applied at the ends of channels $2^{(1)}$ and $2^{(2)}$ (Fig. 3), relative to that in channel $1^{(1)}$, as a function of the relative electrokinetic potential. The *curves* denote the values required to attain $Q_2^{(1)} = Q_2^{(2)} = 0$, while the flow is established from channel $1^{(1)}$ toward channel $1^{(2)}$. Vertical (*dotted*) lines indicate potential values corresponding to different plots in Fig. 5

(Fig. 3). Coefficients L_{11}, L_{12}, and L_{22} for every channel were evaluated from Eqs. (7), (8), and (12), respectively. In Eq. (7), the first five terms of the series were used (the sum equals 0.748 for $w/h = 2.5$).

The following simple operation is simulated here: the electrolyte solution is transported from channel $1^{(1)}$ towards channel $1^{(2)}$ by applying an appropriate potential difference between channels ends, for example $V_1^{(1)} = 500$ V and $V_1^{(2)} = 0$. Electric potentials are also applied to the ends of branches $2^{(1)}$ and $2^{(2)}$ in order to avoid leakage; that is, side arms are "pinched" (Dodge et al. 2001). For simplicity, the condition $Q_2^{(1)} = Q_2^{(2)} = 0$ is imposed here. The main feature to be discussed is that, because microchannels are heterogeneous in surface properties ($\zeta_{RC} \neq \zeta$), finite pressures develop at the junctions. The effect is well known in the literature, mainly in relation with micropumping (e.g. Chien and Bousse 2002). As a consequence, the potentials $V_2^{(1)}$ and $V_2^{(2)}$ required to maintain the condition $Q_2^{(1)} = Q_2^{(2)} = 0$ depend on the ratio ζ_{RC}/ζ, as shown in Fig. 4. The curves in this figure define a sort of operation diagram, which is of interest in the design and manipulation of the microreactor.

Furthermore, these pressure gradients strongly affect the flow field in each channel. In order to examine flow details in the reaction chamber, $u_z(x,y) = u_z^{(p)}(x,y) + u_z^{(e)}$ can be plotted from Eqs. (5) and (6), considering that pressure and potential values at junctions 1 and 2 were calculated beforehand. Thus Fig. 5 shows the velocity profiles for different values of ζ_{RC}, while $\zeta = -60$ mV. It is observed that the flat profile associated with pure electro-osmotic flow (Fig. 5a) is only attained when channels are perfectly homogeneous in surface properties. If $\zeta_{RC} > \zeta$, a pressure gradient is generated in the direction of the flow (Fig. 5b). In particular, this case emulates a practical situation found in the experiment of Dodge et al. (2001), where $\zeta \approx -60$ mV and $\zeta_{RC} \approx -20$ mV. Instead, if $\zeta_{RC} < \zeta$, the pressure gradient has the opposite direction (Fig. 5c).

An interesting aspect to observe is that, although the overall flow in the reaction chamber is always established from junction 1 towards junction 2, the fluid velocity on the walls varies in magnitude, being even negative when $\zeta_{RC} > 0$ (Fig. 5d). These results offer relevant information to be considered in the optimization of reactions that take place on channel walls, such as the immunoreactions involved in the analytical chips mentioned above. In fact, analytes are transported by the electrokinetic flow to reach binding sites on the reactive channel wall; hence the rate of surface reactions depends on the fluid velocity profile (see, for example, Gervais and Jensen 2006).

7 Concluding remarks

Electrokinetically driven microfluidic networks may be described by analogy with electrical circuits, provided a series of conditions are satisfied. The equivalent circuit model discussed here is able to predict the simultaneous flows of fluid and electricity in the entire network, for a given configuration of the applied pressures and electric potentials. As stated by Erickson (2005), the development of these techniques is an important step to achieve numerical simulation of whole microfluidic chips.

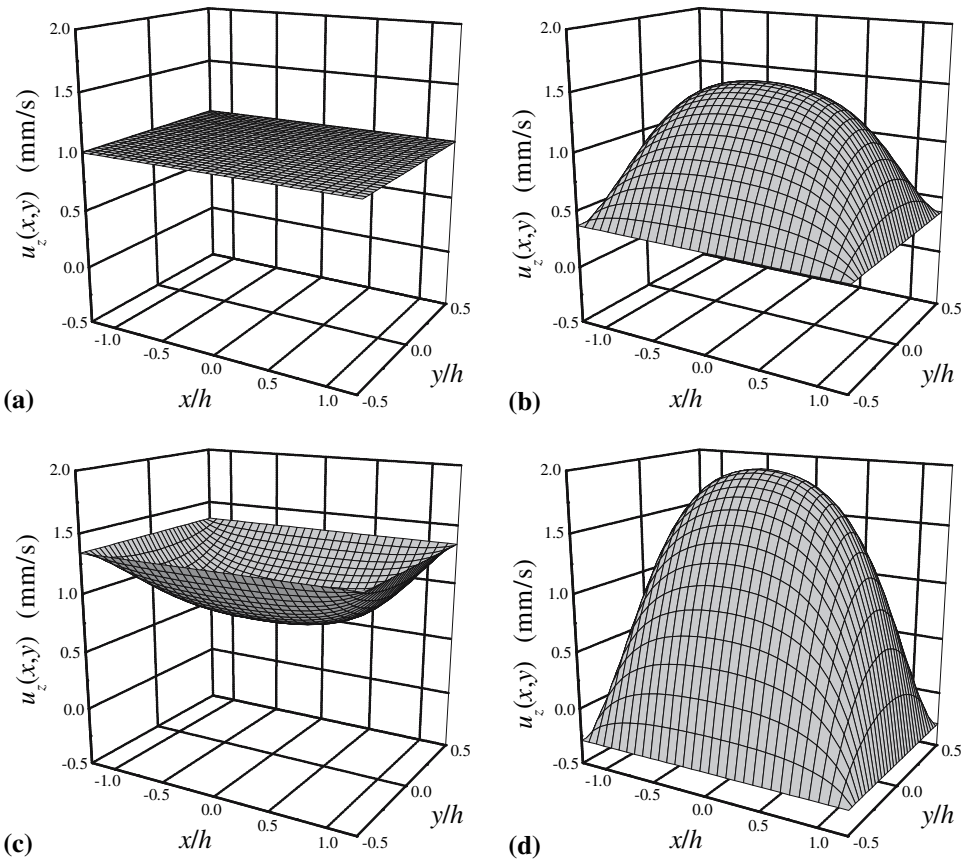

Fig. 5 Fluid velocity in the reaction chamber of the double T-shaped microreactor (Fig. 3, from bottom to top), for different values of the surface potential ζ_{RC}: **a** –60, **b** –20, **c** –80, and **d** +20 mV. In all cases, ζ = –60 mV, $V_1^{(1)}$ = 500 V, and $V_1^{(2)}$ = 0. Potentials $V_2^{(1)}$ and $V_2^{(2)}$ are those indicated in Fig. 4 for the respective values of ζ_{RC}/ζ

The conductance coefficients of rectangular microchannels were derived under the thin EDL approximation, mainly to attain analytical equations. In fact, the evaluation of the electrokinetic flow in rectangular microchannels with arbitrary values of λ requires numerical calculations (e.g. Li 2004). This complexity could be conveniently avoided here because the model is addressed to analytical chips, where Debye lengths hardly reach 10 nm, whereas channel depths are normally higher than 10 μm. Actually $\lambda < 10^{-4}\,h$ in the practical examples discussed above.

Furthermore, a detailed analysis of electro-osmosis and streaming effects in rectangular microchannels was carried out, to clearly identify the range of validity of all assumptions made, and the consequent limitations of the model. At a first view, it may appear that the large number of conditions outlined in Sect. 4 leaves few possibilities to use equivalent circuit models in real systems. Nevertheless, analytical devices operated by electrokinetic flow satisfy most of these requirements. As a relevant example, it was shown how the model successfully matches data corresponding to an electrokinetically controlled chip for immunoassays (Hu et al. 2005).

Finally, based on the simulations discussed in the last section one may conclude that, apart from the valuable assistance in manipulations, well formulated circuit models can certainly help to design and optimize analytical microsystems.

Acknowledgments The author wishes to thank Agencia Nacional de Promoción Científica y Tecnológica and Consejo Nacional de Investigaciones Científicas y Técnicas, Argentina, for the financial aid received.

References

Berli CLA (2007) Theoretical modelling of electrokinetic flow in microchannel networks. Colloids Surf A Physicochem Eng Asp 301:271–280

Brody JP, Yager P, Goldstein RE, Austin RH (1996) Biotechnology at low Reynolds numbers. Biophys J 71:3430–3441

Brunet E, Adjari A (2004) Generalized Onsager relations for electrokinetic effects in anisotropic and heterogeneous geometries. Phys Rev E 69:016306

Brunet E, Adjari A (2006) Thin double layer approximation to describe streaming current fields in complex geometries: analytical framework and applications to microfluidics. Phys Rev E 73:056306

Chatterjee AN, Aluru NR (2005) Combined circuit/device modeling and simulation of integrated microfluidic systems. J Microelectromech Syst 14:81–95

Chiem NH, Harrison DJ (1998) Microchip systems for immunoassay: an integrated immunoreactor with electrophoretic separation for serum theophylline determination. Clin Chem 44:591–598

Chien R-L, Bousse L (2002) Electroosmotic pumping in microchips with non-homogeneous distribution of electrolytes. Electrophoresis 23:1862–1869

Cummings EB, Griffiths SK, Nilson RH, Paul PH (2000) Conditions for similitude between the fluid velocity and electric field in electroosmotic flow. Anal Chem 72:2526–2532

De Groot SR (1951) Thermodynamics of irreversible processes. North-Holland, Amsterdam

Dodge A, Fluri K, Verpoorte E, de Rooij NF (2001) Electrokinetically driven microfluidic chips with surface-modified chambers for heterogeneous immunoassays. Anal Chem 73:3400–3409

Erickson D (2005) Towards numerical prototyping of labs-on-chip: modeling for integrated microfluidic devices. Microfluid Nanofluid 1:301–318

Fletcher PDI, Haswell SJ, Paunov VN (1999) Theoretical considerations of chemical reactions in micro-reactors operating under electroosmotic and eletrophoretic control. Analyst 124:1273–1282

Gervais T, Jensen KF (2006) Mass transport and surface rections in microfluidic systems. Chem Eng Sci 61:1102–1121

Geyer PE, Rosaguti NR, Fletcher DF, Haynes BS (2006) Thermohydraulics of square-section microchannels following a serpentine path. Microfluid Nanofluid 2:195–204

Hu G, Gao Y, Sherman PM, Li D (2005) A microfluidic chip for heterogeneous immunoassay using electrokinetical control. Microfluid Nanofluid 1:346–355

Hunter RJ (1992) Foundations of colloid science, vols. I and II. Clarendon Press, Oxford

Knight JB, Vishwanath A, Brody JP, Austin RH (1998) Hydrodynamic focusing on a silicon chip: mixing nanoliters in microseconds. Phys Rev Lett 80:3863–3866

Kohlheyer D, Besselink GAJ, Lammertink RGH, Schlautmann S, Unnikrishnan S, Schasfoort RBM (2005) Electro-osmotically controllable multi-flow microreactor. Microfuid Nanofluid 1:242–248

Li D (2004) Electrokinetics in microfluidics. Elsevier, London

MacInnes JM, Du X, Allen RWK (2003) Prediction of electrokinetic and pressure flow in a microchannel T-junction. Phys Fluids 15:1992–2006

Morf WE, Guenat OT, de Rooij NF (2001) Partial electroosmotic pumping in complex capillary systems. Part 1: principles and general theoretical approach. Sens Actuators B 72:266–272

Probstein RF (1989) Physicochemical hydrodynamics. Butterworths, New York

Rastogi RP, Srivastava RC, Singh SN (1993) Nonequilibrium thermodynamics of electrokinetic phenomena. Chem Rev 93:1945–1990

Seiler K, Fan ZH, Fluri K, Harrison DJ (1994) Electroosmotic pumping and valveless control of fluid flow within a manifold of capillaries on a glass chip. Anal Chem 66:3485–3491

Squires TM, Quake SR (2005) Microfluidics: fluid physics at the nanoliter scale. Rev Mod Phys 77:977–1026

Stone HA, Stroock AD, Adjari A (2004) Engineering flows in small devices: microfluidics toward lab-on-a-chip. Annu Rev Fluid Mech 36:381–411

Tabeling P (2005) Introduction to microfluidics. Oxford University Press, New York

White FM (1975) Viscous fluid flow. McGraw-Hill, New York

Xuan X, Li D (2004) Analysis of electrokinetic flow in microfluidic networks. J Micromech Microeng 14:290–298

Yang R-J, Fu L-M, Hwang C-C (2001a) Electroosmotic entry flow in a microchannel. J Colloid Interface Sci 244:173–179

Yang R-J, Fu L-M, Lin Y-C (2001b) Electroosmotic flow in microchannels. J Colloid Interface Sci 239:98–105

Zhou T, Liu A-L, He F-Y, Xia X-H (2006) Time-dependent starting profile of velocity upon application of external electrical potential in electroosmotic driven microchannels. Colloids Surf A Physicochem Eng Asp 277:136–144